EPJ Web of Conferences **26**, 02013 (2012)
DOI: 10.1051/epjconf/20122602013


# The influence of peak shock stress on the high pressure phase transformation in zirconium

E.K. Cerreta, J.P. Escobedo, P.A. Rigg, F.L. Addessio, T. Lookman, C.A. Bronkhorst, C.P. Trujillo, D.W. Brown, P.O. Dickerson, R.M. Dickerson, and G.T. GrayIII

*Los Alamos National Laboratory, Los Alamos, New Mexico 87544, USA*

**Abstract.** At high pressures zirconium is known to undergo a phase transformation from the hexagonal close packed (HCP) alpha phase to the simple hexagonal omega phase. Under conditions of shock loading, the high-pressure omega phase is retained upon release. However, the hysteresis in this transformation is not well represented by equilibrium phase diagrams and currently models that accurately represent such a solid-solid phase transformation coupled with the multi-phase plasticity likely under shock conditions do not exist. For this reason, the influence of peak shock stress on the retention of omega phase in Zr is explored in this study. In-situ VISAR measurements along with post-mortem metallographic and neutron diffraction characterization of soft recovered specimens have been utilized to quantify the volume fraction of retained omega phase, morphology of the shocked alpha and omega phases, and qualitatively understand the kinetics of this transformation. This understanding of the role of peak shock stress will be utilized to address physics to be encoded in our present macro-scale models.

## 1 Introduction

Under shock loading conditions, zirconium has been observed to undergo a phase transformation from the hexagonal close packed (HCP) $\alpha$-phase to the simple hexagonal $\omega$-phase [1,2]. This phase transformation has been shown to display a hysteretic behavior [3,4]. Specifically, upon shock-loading zirconium to stresses in excess of the phase transformation stress (7 GPa) and then unloading to ambient pressure, soft-recovered specimens have been observed to retain high fractions of meta-stable omega phase, as much as 40% [5]. Many studies have been performed to examine this behavior. These studies have primarily focused on determining the pressure for the phase transformation, crystallography of the transformation, subsequent mechanical properties, and electronic structure calculations [6–9]. While these studies reported numerous orientation relationships between the $\alpha$ and $\omega$-phases, almost all indicate that the $\omega$-phase exists as a fine-scale precipitate, on the order of nanometers in size, within the $\alpha$-phase grains.

Even though the post-mortem nature of the retained $\omega$-phase has been characterized, there are a number of unaddressed questions with regard to this high-pressure phase transformation. For example, few studies have focused on the role of peak shock stress, temperature at which the material was tested, and the kinetics of the release from peak stress on the hysteresis of the phase transition, even though these parameters are suspected to have an influence on this response.

Currently, material models are not nearly sensitive enough to microstructural or chemical composition information to enable predictive representation of non-equilibrium and extreme event processes such as phase transformation under dynamic loading conditions. Traditional polycrystal models have been based on heterogeneous response at the multi-crystal length scale but have relied on continuum single crystal theories, which incorporate plastic deformation processes like dislocation slip and twinning in a highly homogenized and phenomenological way. A robust model for high-pressure phase transformations would account for the coupled physical processes of plasticity and solid-solid phase transformations in materials. To do this, the hysteresis and meta-stability of the $\alpha$ to $\omega$-phase transition needs to be characterized in a way that determines microstructure and allows for the development of models that are not based on the concept of an "equilibrium" phase boundary. As such, the phase diagram under dynamic conditions, with hysteretic windows, must be mapped and microstructure evolution due to phase change, damage, deformation twinning and plasticity understood.

To this end, a study has been performed to examine the hysteresis of the high-pressure phase transformation in high-purity zirconium and characterize the shock-deformed microstructure as a function of peak shock stress. Plate impact experiments have been conducted to peak shock stresses of 8 and 10.5 GPa at room temperature. These pressures were chosen as they are above that typically reported for the $\alpha$ to $\omega$ transition [5]. In-situ particle velocity measurements were made using a VISAR diagnostic and all specimens were soft recovered for post-mortem metallographic analysis. Multi-scale characterization of the alpha and omega phase orientation relationship and substructural evolution was performed via optical metallography, electron back scattered diffraction (EBSD) and transmission electron microscopy (TEM). Quantitative measurements of the volume fraction of omega phase retained upon unloading and the texture evolution of the $\alpha$-phase were performed via neutron diffraction.

The results of this study indicate that peak shock stress as well as crystal orientation with respect to the shock direction is an important consideration for the $\alpha$ to $\omega$ high-pressure phase transformation. These data yield insight toward an advanced understanding of the dynamic rather than equilibrium phase diagram for Zr and in this way lend important constraints for the development of phase aware strength and damage models.

**Table 1.** Chemistry of the Zr Alloy in wr% PPM.

| Material | O | C | N | Al | V | Fe |
|---|---|---|---|---|---|---|
| High Purity Zr | <50 | 22 | <20 | <20 | <50 | <50 |

## 2 Experimental

This investigation was performed on high-purity, crystal bar grade Zr. Table 1 gives the chemistry for this material and processing details are provided elsewhere [5]. To investigate the influence of peak shock stress on $\omega$-phase formation, wave profile and shock recovery experiments were conducted. All shock recovery experiments were performed on an 80 mm-single-stage launcher utilizing a shock assembly consisting solely of Zr and the wave profiles were measured with a VISAR built at Los Alamos [10]. The precision of the wave velocity measurements is estimated to be approximately 1% in particle velocity. Photomultiplier circuits were utilized that had a 1 ns rise time.

Optical and electron microscopy as well as neutron diffraction was performed to characterize the as-annealed and shocked materials. Electron back-scattered diffraction was performed on a Philips XL30. TEM was performed on an FEI Tecnai F30 Analytical TEM/STEM. Neutron diffraction experiments were performed on the High Intensity Powder Diffraction (HIPD) instrument at the Los Alamos Neutron Scattering Center (LANSCE). Bulk specimens were examined without special preparation because the neutron penetration is large enough to sample the entire specimen.

## 3 Results and discussion

### 3.1 Velocimetry

The shock-wave-profile experiments conducted on Zr were performed to quantify the pressure of the $\alpha$ to $\omega$-phase transition as a function of peak shock stress. Experiments were performed to peak shock stresses of 8, 10.5, and 12 GPa. The shock-wave profiles measured using VISAR are given in Fig. 1. From this figure the $\alpha$ to $\omega$-phase transition is identified by arrows for each shock profile. However the stress for the transformation is lower for the 8 GPa experiment than it is for the 10.5 and 12 GPa experiments. Additionally the rise time to the peak stress after the phase transformation differs as a function of peak stress. The quickest rise time to the peak shock stress is observed in the 12 GPa case and 10.5 GPa experiment shows a relatively slower rise time to the peak shock stress. In the case of the 8 GPa experiment, the slowest rise time is observed. This result is consistent with the idea that for high purity Zr, the kinetics of the phase transformation are significantly influenced by the drive conditions. Finally, the lack of a rarefaction shock in all cases suggests that no reverse phase transformation occurred. Instead, upon recovery of the specimen, meta-stable $\omega$-phase should be retained.

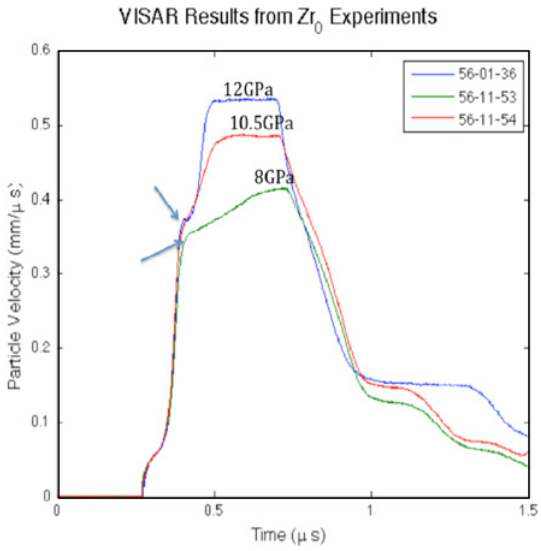


**Fig. 1.** VISAR data for each of the three shock experiments. Arrows indicate the onset of the $\alpha$ to $\omega$-phase transformation.

### 3.2 Neutron diffraction analysis

Neutron diffraction experiments were performed on Zr specimens shock loaded to peak shock stresses of 8 and 10.5 GPa and soft recovered. All data from shocked experiments was compared against an as-annealed, high purity Zr standard. From these experiments both the texture evolution within the $\alpha$ and $\omega$-phases and the volume fraction of $\omega$-phase was determined. This analysis revealed that within the soft recovered specimens 63% and 82% $\omega$-phase was retained within the Zr after release from peak stresses of 8 and 10.5 GPa, respectively. It should be noted that this is significantly higher than values within the literature for similar experiments [5]. At this point, without an in-situ measurement of the volume fraction of phase transformed material while under the peak shock stress, there is no way to know if these specimens ever were 100% $\omega$-phase and if the experiments were able to retain all of the phase transformed product upon release. However, if 100% $\omega$-phase was achieved in each test, it is likely that the rate at which these specimens were released could influence the retention of the high-pressure phase. Higher release rates associated with the higher peak stress experiment, would likely leave less time for reversion or "quench in" more of the high-pressure phase than the lower peak shock stress experiments.

Texture evolution of the $\alpha$-phase is shown in pole figures provided in Fig. 2. While the initial texture of the as-annealed material has a strong basal pole fiber, the shocked materials display significant rotation of this fiber away from the basal pole texture. Previously, it has been shown that significant texture reorientation in $\alpha$-phase Zr can occur through twinning promoted during high rate deformation [11]. However, typically twin systems activated upon shock loading lead to a 90° rotation of the basal pole [12]. This rotation is not observed in the present study. This may be due to the fact that the low volume fractions of $\alpha$-phase that exist after shock do not lend themselves to generating the high intensities necessary to characterize

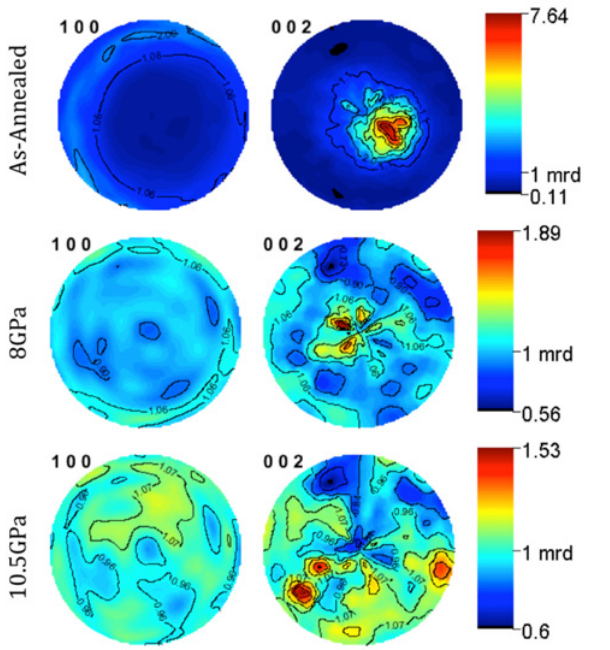


**Fig. 2.** Neutron diffraction generated $\alpha$-phase pole figures for the as-annealed as well as the 8 and 10.5 GPa shock loaded, high purity Zr.

this rotation of the 0001 basal pole by tensile twinning. It may also suggest that the twin volumes are more prone to $\omega$-phase transformation than the parent $\alpha$-phase volumes, and therefore these twinned and then transformed volumes of material do not contribute to the $\alpha$-phase texture in the post mortem analysis. Finally, the $\omega$-phase pole figures, not shown here, display nearly random textures.

### 3.3 Post mortem metallographic analysis

Optical metallography, hardness testing, EBSD, and TEM were utilized to characterize the post-mortem microstructures. Optical analysis of the shock-loaded specimens is shown in Fig. 3 and the microstructures are compared with the as-annealed Zr microstructure. It can be seen from Fig. 3 that both shock-deformed microstructures are dominated by twinning. Multiple twins and sometimes multiple twin variants were activated within almost all grains in the shock deformed microstructures.

To differentiate between the $\alpha$ and $\omega$-phases, EBSD was utilized. Figure 4 shows image quality (IQ) and inverse pole figure (IPF) maps for both phases in the 8 and 10.5 GPa specimens. The IQ maps show the significant amount of deformation present in both specimens as each microstructure appears to be heavily twinned. Figures 4(c) and 4(g) show the substantial volume fraction of $\omega$-phase within the shock-loaded microstructures of both specimens as only the $\omega$-phase was imaged in these figures. Figures 4(d) and 4(h) show the morphology of the $\alpha$-phase within these specimens. The $\alpha$-phase consists mostly of laths within the $\omega$-grains, which appear black in these images as only $\alpha$-phase was imaged for these figures. While these laths may have a similar morphology to twins, they likely represent volumes of material that did not twin prior

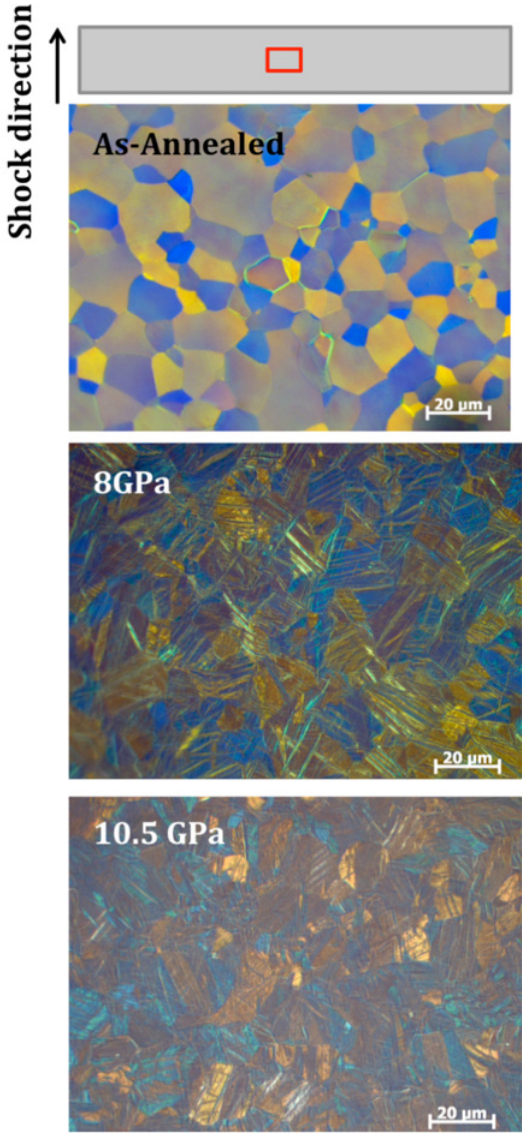


**Fig. 3.** Optical images of the as-annealed as well as the 8 and 10.5 GPa specimens. At the top of the figure a schematic shows from where in the soft recovered and cross-sectioned specimens, the images were taken as well as the shock loading direction.

to the phase transformation. Metallographic and texture analysis of specimens shock loaded to peak stresses below that for the phase transformation, indicate that twinning is substantial. Additionally, for the grains that do twin, most of the grain is consumed by the growing deformation twin [13–15]. Only thin laths of parent grain are left in these cases. Such laths are consistent with the thicknesses of the $\alpha$-phase laths shown in Figs. 4(d) and 4(h). This, along with the neutron diffraction results displaying a lack of texture in the shocked $\alpha$-phase, suggest that the $\omega$-phase transition may be promoted in twinned $\alpha$-phase material as compared to parent phase material within the same grain. This observation gives an insight for an orientation dependence of this phase transformation relative to the imposed shock-loading direction.

Hardness testing on the soft recovered, shock loaded specimens was utilized to gain insight into the strength of

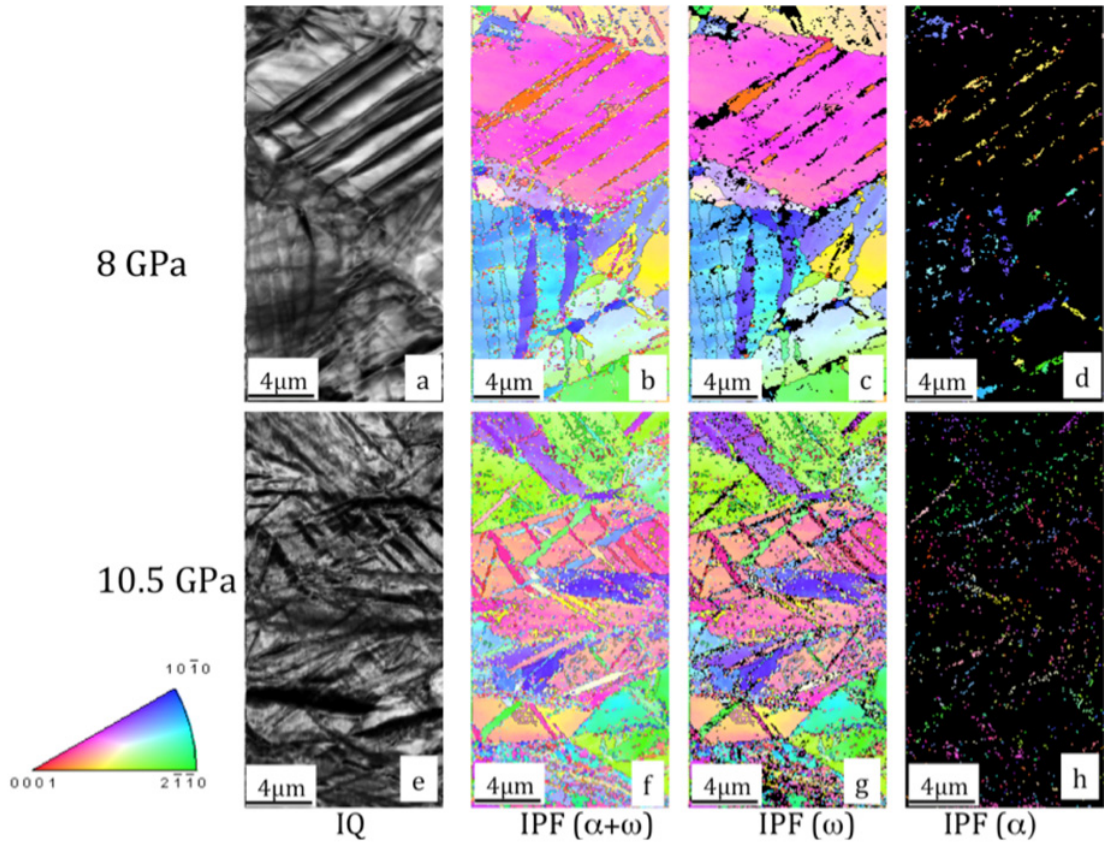


**Fig. 4.** EBSD generated maps of the shock loaded 8 GPa and 10.5 GPa specimens. At 8 GPa the (a) image quality (IQ) map, (b) inverse pole figure (IPF) map showing both $\alpha$ and $\omega$-phases, (c) IPF map for just the $\omega$-phase, and (d) the IPF map for just the $\alpha$-phase are given. At 10.5 GPa the (e) IQ map, (f) IPF map showing both $\alpha$ and $\omega$-phases, (g) IPF map for just the $\omega$-phase, and (h) the IPF map for just the $\alpha$-phase are given.

the $\omega$-phase. While neither specimen was 100% $\omega$-phase, hardness measurements were used as an indirect way to assess the strength of the $\omega$-phase through measurements of the $\alpha$ and $\omega$-phase composite specimens and then comparing those results with Zr material that is in the as-annealed as well as the significantly deformed condition. Figure 5 gives hardness data for a number of Zr specimens. These data include Zr that is in the as-annealed; the heavily twinned; the sheared; the sheared and recrystallized; and finally the sheared, recrystallized, and annealed conditions. These data have been provided to compare hardness measurements on the shocked specimen, which experienced both deformation and the high-pressure phase transformation, with this anticipated in Zr that is just severely deformed. It can be seen from these data that hardness values rise steadily for materials tested to increasing levels of deformation (30, 100, and 300% strain). Recrystallization and annealing of course significantly decrease the measured hardness values of the material. However, there is a significant jump in hardness data for specimens that have been shock loaded above the $\alpha$ to $\omega$ phase transition. These hardness values are significantly higher even as compared to Zr specimens deformed to 300% strain, which have been shown to store high dislocations densities within specimens as well as to be appreciably twinned [16, 17]. This suggests that either one or a combination of factors lead to enhanced strength in the shock-deformed material. These factors are not limited to, but could include (1) the possibility that the $\omega$-phase has a higher yield stress than the $\alpha$-phase; (2) dislocation densities to accommodate $\omega$-phase formation are substantial enough to harden the shocked specimen even over other highly deformed materials, and/or (3) dislocation glide distances available within the shocked material are reduced because of the morphology of the $\omega$-phase precipitates within the $\alpha$-phase. The smaller c/a ratio of the $\omega$-phase as compared to the $\alpha$-phase is consistent with higher shear stresses to activate slip in the $\omega$-phase and therefore a higher yield stress than the $\alpha$-phase [2].

Transmission electron microscopy (TEM) analysis of the shock deformed substructure of both the 8 and 10.5 GPa specimens was utlized to evaluate the contributions of the reduced glide distances and stored dislocation substructure. Initial work, shown in Fig. 6, reveals that the density of stored defects in the shock loaded microstructures is quite high. This is evidenced by the significant amount of contrast in the bright field image given in Fig. 6. Interestingly, high angle annular dark field (HAADF) images of the shocked microstructure, Fig. 7, show laths similar to those imaged as $\alpha$-phase in Fig. 4(h). In the HAADF mode, material with less strain appears darker. Since the darker material is the lath structure, this figure along with Fig. 4(h) suggests that most of the stored defect content resides in the $\omega$-phase.

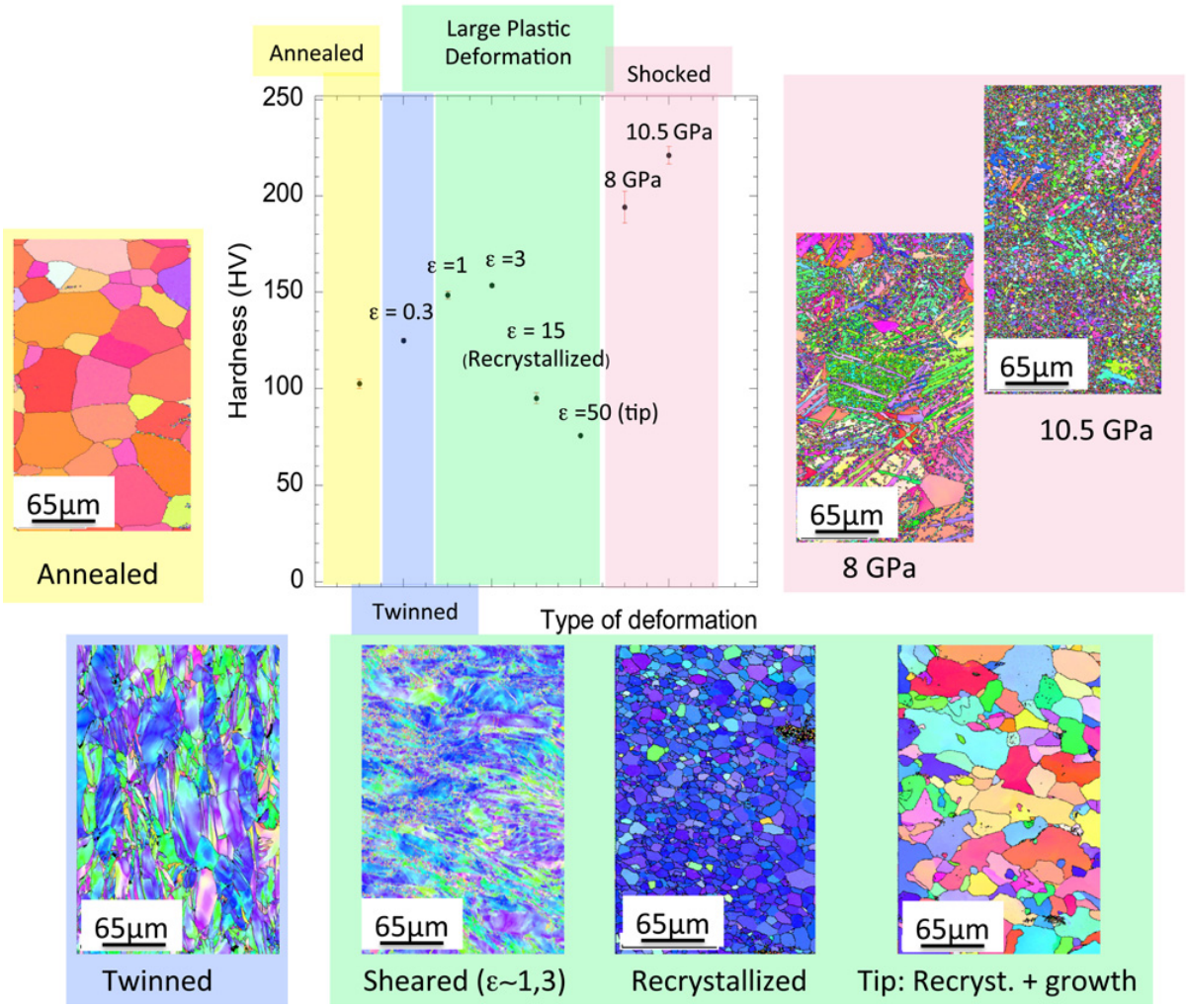


**Fig. 5.** EBSD generated IPF maps for as-annealed, heavily twinned, sheared, sheared and recrystallized, and sheared, recrystallized, and annealed, as well as 8 and 10.5 GPa shock loaded specimens. Micro-hardness data as a function of the deformation type is given.

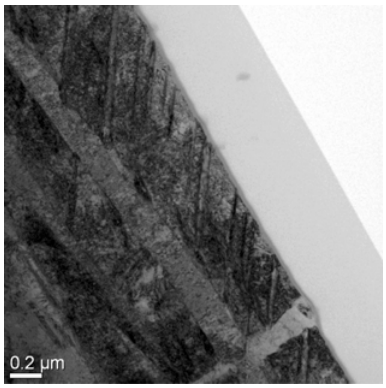


**Fig. 6.** Bright field image of the 10.5 GPa specimen showing the significant amount of stored defects within the substructure.

## 4 Summary

In this study, the initial experimental work to probe the hysteresis of the $\alpha$ to $\omega$-phase transition as a function of peak shock stress has been presented. This work has revealed the following with regard to this phase transformation:

1) The kinetics of the $\alpha$ to $\omega$-phase transformation is highly dependent on the stress history applied even for the narrow range of peak stress states and rates of loading applied in this study.
2) By adjusting the peak stress achieved during shock loading, the drive condition applied to the sample was changed such that the amount of retained $\omega$-phase was higher in specimens loaded to higher peak shock stresses.
3) Post-mortem metallographic analysis suggests that the $\omega$-phase transformation is preferred in the twinned $\alpha$-phase. This may be the signature of an orientation dependent transformation.
4) The hardness values associated with shock-loaded specimens suggest that the $\omega$-phase strengthens Zr. TEM analysis suggests that the significant stored defect density in the $\omega$-phase contributes to this.

Future work will also include examination of the role of temperature on the $\alpha$ to $\omega$-phase transition and specifically on the retention of $\omega$-phase after release from the peak shock stress.

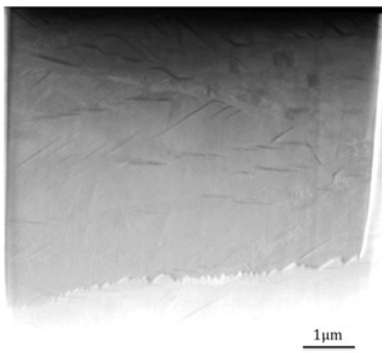


**Fig. 7.** HAADF image of the 10.5 GPa specimen.

## Acknowledgements

Los Alamos National Laboratory is operated by Los Alamos National Security, LLC, for the National Nuclear Security Administration of the U.S. Department of Energy under contract DE-AC52-06NA25396. This work was partially sponsored by the Joint DoD/DOE Munitions Technology Development Program.

## References

1. C. Greeff, D. Trinkle, R. Albers: J. Appl. Phys. **90**, 2221 (2001)
2. S. K. Sikka, Y. K. Vohra, R. Chidambaram: Prog. Mat. Sci. **27**, 245 (1982)
3. J. C. Jamieson: Science **140**, 72 (1963)
4. G. T. Gray, In: *Shock Wave And High Strain Rate Phenomena in Materials*, edited by Meyers M, Murr LE, Staudhammer KP, Marcel Dekker Inc., NY(1992), p.899
5. E. Cerreta, G. T. Gray, R. Hixson, P. A. Rigg, D. W. Brown: Acta Mat. **53,** 1751 (2005)
6. P. A. Rigg, C. W. Greef, M. D. Knudson, D. Hayes, R. Hixson, G. T. Gray, *13th Annual Symposia on Shock Compression of Condensed Matter*(American Physical Society, 2003)
7. A. Rabinkin, M. Talianker, O. Botstein: Acta Metal. **29**, 691 (1981)
8. E. Cerreta, G. T. Gray, B. Henrie, D. W. Brown, R. Hixson, P. A. Rigg, *Shock Compression of Condensed Matter-2003* (AIP, 2003)
9. R. G. Hennig, D. R. Trinkle, J. Bouchet, S. G. Srinivasan, R. C. Albers, J. W. Wilkins: Nature of Materials 129 (2005)
10. W. Hemsing: Rev. Sci. Inst. **50**, 73 (1979)
11. G. C. Kaschner, G. T. Gray: Metal. Mat. Trans. A **31,** 1997 (2000)
12. J. F. Bingert, T. A. Mason, G. C. Kaschner, P. J. Maudlin, G. T. Gray: Metal. Mat. Trans. A **33**, 955 (2002)
13. I. Beyerlein, L. Capolungo, P. Marshall, R. McCabe, C. N. Tome: Phil. Mag. **90**, 4073 (2010)
14. R. J. McCabe, G. Proust, E. K. Cerreta, A. Misra: Int. J. Plas. **25**, 454 (2009)
15. B. Henrie, T. A. Mason, B. Hansen: Metal. Mat. Trans. A **35**, 3745 (2004)
16. J. Escobedo, E. K. Cerreta, C. Trujillo, D. Martinez, G. T. Gray, R. A. Lebensohn, V. Webster: Acta Mat. (to be published)
17. C. Trujillo, J. Escobedo, G. T. Gray, E. K. Cerreta, D. Martinez: Dynamic Behavior of Materials **1**, 467 (2011)